Title
SOME ASPECTS OF STRONGLY HEATED TURBULENT BOUNDARY LAYER FLOW

Authors
Cheng, R.K.
Ng, T.T.

Publication Date
1981-11-01

LBL-13549
Preprint

Lawrence Berkeley Laboratory
UNIVERSITY OF CALIFORNIA

ENERGY & ENVIRONMENT
DIVISION

Submitted to The Physics of Fluids

SOME ASPECTS OF STRONGLY HEATED TURBULENT BOUNDARY LAYER FLOW

R.K. Cheng and T.T. Ng

November 1981

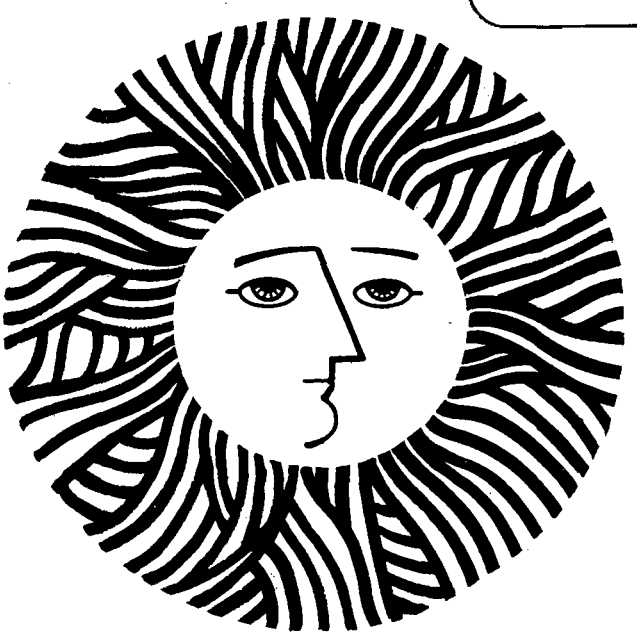

Prepared for the U.S. Department of Energy under Contract W-7405-ENG-48

DISCLAIMER

SOME ASPECTS OF STRONGLY HEATED TURBULENT BOUNDARY LAYER FLOW

R.K. Cheng and T.T. Ng

Lawrence Berkeley Laboratory
University of California, Berkeley
Berkeley, California 94720

This work was supported by the Director, Office of Energy Research, Office of Basic Energy Sciences, Chemical Sciences Division of the U.S. Department of Energy under contract No. W-7405-ENG-48. Additional equipment was supported by AFOSR Contract F 446-20-76-C-0083 through the Office of Research Services, University of California, Berkeley.

SOME ASPECTS OF STRONGLY HEATED TURBULENT BOUNDARY LAYER FLOW

R.K. Cheng and T.T. Ng

Lawrence Berkeley Laboratory
University of California, Berkeley
Berkeley, California 94720

ABSTRACT

Rayleigh scattering and laser Doppler velocimetry were used to study density and velocity statistics in a strongly heated turbulent boundary layer with free stream velocity U =19m/s and wall temperature T_w =1100K. Mean and rms fluctuation profiles of density and velocity were found to be self preserving, and the velocity profiles were not significantly affected by wall heating. Streamwise velocity profiles, and mean temperature profiles deduced from density data were compared with Townsend's self preserving analysis. It was found that wall heating caused a reduction in Reynolds stress within the thermal layer. This phenomenon was explained with reference to the thermal layer structures observed in high speed schlieren movies.

Nomenclature

H	shape factor of boundary layer, δ_d/δ_m
Q_w	heat flux at the wall
Re_x	Reynolds number
S_t	Stanton number
T(t)	temperature; T,time mean value; θ ,turbulence component.
t	time
U(t)	streamwise velocity-- U, time mean value; u, turbulent component, u'; rms fluctuation
u^+	normalized streamwise velocity, U/u_τ
u_τ	stress velocity

$-\overline{uv}$	Reynold stress
V(t)	cross-stream velocity— V, time mean value; v, turbulence component; v′, rms fluctuation
x	streamwise coordinate
y	cross-stream coordinate
y^+	normalizes cross-stream coordinate = $y\, u_\tau / \nu$
δ_d	displacement thickness = $\int_0^\infty \left(1 - \frac{\rho U}{\rho_\infty U_\infty} \right) dy$
δ_h	enthalpy thickness = $\int_0^\infty \frac{\rho U}{\rho_\infty U_\infty} \left(\frac{T_w - T}{T_w - T_\infty} \right) dy$
δ_m	momentum thickness = $\int_0^\infty \frac{\rho U}{\rho_\infty U_\infty} \left(1 - \frac{U}{U_\infty} \right) dy$
δ_u	velocity boundary layer thickness at $U/U_\infty = 0.99$
δ_T	thermal boundary layer thickness at $\rho/\rho_\infty = 0.99$
ν	kinematic viscosity
$\rho(t)$	density; ρ, time mean value; ρ' , rms fluctuation
θ_τ	friction temperature; Q_w/u_τ

1. Introduction

One of the fundamental flow configurations for heat transfer and fluid mechanics studies is the turbulent boundary layer flow over a heated flat surface. This configuration is relevant to many engineering and atmospheric applications and has been the subject of a number of experimental and theoretical studies. However, the majority of these studies are focused on cases involving slightly heated surfaces ($\Delta T \leq 20$ K) and are emphasized on determining heat transfer and skin friction coefficients, although there are also some reports on velocity and temperature statistics. Johnson[1], Blom[2], and Antonia[3] et. al. measureed velocity and temperature, and some of their cross and triple correlations. Based on self preservation analysis, Townsend[4] developed a set of empirical equations for the temperature and velocity profiles. These equations agreed reasonably well with experimental data[3].

Relatively minor attention has been given to the study of the turbulent boundary layer flow over strongly heated surface in which significant density variations are produced. One of the reasons is that conventional hot-wire and thermocouple data obtained in this environment are difficult to interpret. Consequently, there are only a few publications on this boundary layer flow and these experimental data are insufficient to characterize the mechanisms responsible for momentum and heat transport in the thermal layer. The papers of Nicholl[5] and Rotta[6] are two examples of experimental studies of strongly heated turbulent boundary layer flows.

Nicholl[5] investigated the dynamic effects of density gradients on turbulent structures in turbulent boundary layers over the floor and

roof of a wind tunnel, with the walls heated to 380 K. He reported mean and rms fluctuation profiles of temperature, of two velocity components and also most of the cross-correlations. Floor heating was found to create a local wall jet downstream of the wall temperature discontinuity. This jet was attributed to the vigorous interaction, aided by buoyancy, between the heated air in the thermal layer and the turbulence in the boundary layer. In the heated roof boundary layer, buoyancy stabilized the interface between hot and cold gases and supressed the turbulence.

Rotta[6] conducted an experimental study of heated turbulent boundary layers in air with T_w =523 K and U_∞ of 10 to 30 m/s. His main objective was to deduce analytical profiles for the temperature and velocity distributions. The velocity data were compared with an analytical profile constructed by adding the law of the wall to the law of the wake. This profile is basically Van Driest's compressible turbulent boundary layer profile with the Van Driest constant correlated with the wall heat transfer coefficient. The analytical temperature profile was derived from the analytical velocity profile using the turbulent Prandtl number as an adjustable parameter. These analytical profiles agreed well with most of the experimental data except with the data near the leading edge of the heated plate.

The research reported in this paper is part of a program to study premixed turbulent combustion in boundary layers.[7,8,9] Up to the present, statistical data of turbulent combustion are insufficient to guide the formulation of theoretical numerical models. Many theoretical investigators agree that in addition to studying reacting turbulent

flows, the study of non-reacting turbulent flows with temperature and density gradients of the same order of magnitude as those generated by combustion heat release should be of significance in assisting in the modelling of turbulent transport processes in these highly complex flows.

The objective of the present work is to use laser diagnostics to study the effects of a large stepwise jump in wall temperature on a fully developed turbulent boundary layer. Density (temperature) and two velocity component statistics were obtained with Rayleigh scattering and Laser Doppler Velocimetry (LDV). Results of the velocity measurements in the non-heated turbulent boundary layer are presented in Section 3.2. In Section 3.3, the temperature and velocity profiles in the heated boundary layer are compared with Townsend's self preservation analysis. Also discussed in the same section are the effects of wall heating on the turbulence statistics. Finally in section 4, the evolution of the thermal layer and its interactions with the turbulence structures are discussed with reference to qualitative information obtained from high-speed schlieren movies.

2. Experimental arrangements

The experimental setup is shown schematically in Fig. 1. The turbulent boundary layer is generated over the floor of a 75 cm long by 10 cm square working section of a wind tunnel. The wind tunnel is driven by a 1.12 kw blower providing maximum air speed of 20 m/s. It is mounted on a stepping motor driven three-axis traverse table to enable the scanning of the boundary layer by the stationary laser diagnostic probes. The traverse table is interfaced with a computer controlled

data acquisition system.

The working section consists of three 25 cm long floor segments. The first two segments are enclosed. The third segment which is the heated test section is open to the atmosphere to allow laser diagnostics access. The first segment, immediately downstream of the contraction, is lined with sandpaper to trip the boundary layer. The second segment has a smooth polished aluminum surface. It is maintained at room temperature by a cooling water network installed underneath, since it is in thermal contact with the heated section. The heated test section is a 25 cm extension of the floor of the working section. The heating surface consists of nine 25 mm wide, 0.125 mm thick Kanthal heating strips stretched spanwise across two large ceramic blocks. The heating strips are fitted in recesses milled from the ceramic blocks to provide a flush surface over the entire heated section. They are spaced 2.5 mm apart. Each heating strip is controlled individually by a power supply delivering typically 75 A current at 10 V dc for wall temperature of about 1000 K. The surface temperature was measured by a disappearing filament optical pyrometer with corrections made for the wall emissivity. Details of the heated section design are reported elsewhere[10].

The light source for Rayleigh scattering, LDV and schlieren photography was a Spectra-Physics 4 watt argon-ion laser. For the Rayleigh scattering measurements, the laser beam was focused to a 40 μm waist diameter. Scattered light at the waist was collected at 90^{o} from the beam direction by a lens, filter and photomultiplier assembly. This assembly consisted of a f/1.2, 55 mm focal length camera lens, a 10 nm band pass filter centered at 488 nm and an RCA 931A photomultiplier.

The photomultiplier current was processed by an amplifier with a low pass corner frequency of 5 kHz.

The LDV system consisted of an equal path beam splitter of 5.0 cm fixed separation and a 600 mm focal length lens to form the scattering volume. Aluminum oxide seed particles of 0.3 μm were introduced into the air by a cyclone canister type seeder. Scattering bursts were collected at straight forward direction by a lens, filter photomultiplier assembly. The Doppler bursts were analyzed by a TSI 1090 frequency tracker.

The Rayleigh scattering and LDV systems were interfaced with the computer controlled data acquisition system. The PDP 11/10 computer central to the data acquisition system was programmed to scan the boundary layer automatically at preselected traverse positions. The diagnostic signals were digitized by a 12 bit A/D converter. The progress of the experiments were monitored by plotting the mean values of the signals graphically on a video terminal. Raw data were stored on 7-track magnetic tapes for post processing with the Lawrence Berkeley Laboratory CDC 7600 computer.

The Rayleigh scattering signal was sampled at a rate of 5 kHz and a time series consisting of 8192 samples were digitized at each traverse position. The procedures to remove background intensity from the mean scattering intensity, and electronic noise from the variance of the signal are described in Ref. 9.

As described by Durrani and Greated[11], a single component LDV system can be use to measure two velocity components (U and V) as well as

the Reynolds stress ($-\overline{uv}$). The procedure involves measuring the mean and rms fluctuations of three velocity components at 0^o and $\pm 45^o$ with respect to the x-axis, shown labeled as U, U_1 and U_2 in Fig. 2. This method has been used by Durst et al.[12] Demotakis et al.[13] and in our previous work[14], and was found to be quite satisfactory. With a mean velocity of 20 m/sec, the data rates for all three components were about 20 kHz within most of the boundary layer, dropping to about 8 kHz close to the wall. With these high data rates, it was possible to treat the discrete tracker output as continuous. At each traverse position, a velocity time series of 8192 samples were digitized at a rate of 5 kHz. The boundary layer over each axial station was scanned twelve times to obtain four separate sets of data for each velocity component. The results reported here are the ensemble averages of the four separate measurements. Data reduction methods and noise removal technique were the same as described in Ref. 9.

The schlieren setup consisted of a pair of 75 mm diameter, 1000 mm focal length lenses and a polarization prism used as the schlieren stop. A Fastax rotating prism camera was used to photograph the high speed movies. The maximum framing rate was about 4 kHz which was compatible with the sampling rate for the density and velocity measurements. The development of the thermal layer was studied with three separate movies covering the leading edge, the middle and the end regions of the heated section since the field of view of this setup was limited to 75 mm (i.e the diameter of the schlieren lenses).

3. Results

3.1. The Experiments

All experiments were performed with free stream velocity, U_∞, of 19 m/s, and wall temperature, T_w, of 1100 K. Density and velocity measurements were made at 20 traverse positions over 9 axial stations. The locations of the axial stations are listed in Table 1. Velocity statistics was first measured in the unheated turbulent boundary layer. These results were compared with density and velocity measurements in the heated turbulent boundary layer. The measurements in the heated boundary layer were made after the heated section had been operated for at least 1-1/2 hours to ensure steady state. In general, the wall temperature was fairly uniform except for some cool spots near the edge of the strips. Unfortunately, after the strips were heated for the first time, slight bulges were formed near the center of each strip thus resulting in a less than ideal flat surface over the test section.

The Rayleigh scattering data were reduced to obtain the mean density ρ, rms density fluctuation, ρ', and mean temperature. The velocity data were reduced to obtain two mean velocity components, U and V, their rms fluctuation, u′ and v′, and the Reynolds stress $-\overline{uv}$. Also deduced were several turbulent boundary layer parameters (Table I). The momentum thickness, δ_m, the displacement thickness, δ_d, and enthalpy thickness, δ_h were determined by numerical integration of the mean density and velocity profiles using Simpson's rule. The wall stress velocity, u_τ, was obtained by fitting the law of the wall,

$$\frac{U}{u_\tau} = \frac{1}{K} \ln y^+ + C \qquad (1)$$

using K = 0.41 and C = 5.0. For the heated boundary layer data, the significant density change in the thermal layer was accounted for by the

use of the local coefficient of viscosity to compute y^+.

3.2. The Unheated Turbulent Boundary Layer

The results of velocity measurements in the unheated turbulent boundary layer are compared in this section with those in fully developed turbulent boundary layer. The Reynolds number, Re_x, at the test section, was inferred from the displacement thickness Reynolds number, Re_{δ_d}, since the boundary layer was developed over the contraction and working section of the wind tunnel and had no well-defined origin. The relationship $Re_{\delta_d} = 0.018\ Re_x^{6/7}$ for fully developed turbulent boundary layer was used. The displacement thickness at station 1 was about 1.5 mm (Table 1) which corresponded to $Re_{\delta_d} = 184$ and $Re_x = 7 \times 10^5$. This Reynolds number is just above the level for transition to a fully developed turbulent boundary layer.

Mean streamwise velocity profiles at stations 1, 3, 5 and 7 are shown in Fig. 3 on the logarithmic plot of inner variables u^+ vs. y^+. These profiles agree well with the law of the wall. Their shape factors listed in Table 1 are also consistent with that of a fully developed turbulent boundary layer. Due to the physical limitation of the cross-beam LDV system, the laser probe cannot be placed closer than 1 mm to the wall when measuring U_1 and U_2. This position corresponded to $y^+=59$, therefore our measurements were all made outside of the viscous sublayer.

The rms fluctuation profiles, u' and v', are shown in Fig. 4. The u' profiles are quite consistent whereas the v' profiles are more scattered. The scattered v' data are due to the uncertainties in deducing

v' from u_1', u_2' and u', and the method to remove noise from the variance tends to accentuate the uncertainties at low fluctuation levels.

As pointed out by Willmarth[15] in his review paper on turbulent boundary layers, the rms fluctuation profiles in turbulent boundary layers are not universal. The differences in the profiles are attributed to the differences in the wind tunnel design, free stream turbulence level and also the method of tripping. However, our results agree very well with those of a fully developed turbulent boundary along a rough wall. This should be the consequence of tripping in the working section and the uneven surface over the heating strips. Since the mean and rms fluctuation profiles are quite consistent over the entire test section the boundary layer can be considered as self-preserving.

In Fig. 5, the Reynolds stress profiles are compared with hot-wire measurements[20] within a turbulent boundary layer over smooth surface at $Re_x=7.5x10^4$. Our experimental data are consistent though they do not compare very well with the hot wire profile. Close to the wall, the discrepancy is less with $-\overline{uv}$ reaching to an average of about 80% of the wall shear stress. At the edge of the boundary layer the Reynolds stress data do not decrease to zero. The rms fluctuations at these positions are about 2%. These features at the edge of the boundary layer seem to be characteristics of rough wall turbulent boundary layer. In the outer region, the flow is intermittent and consists of turbulence/laminar flow interface. Tripping at the rough wall could cause some of the turbulence structures to move further out into the free-stream. This would result in higher Reynolds stress and fluctuations at the edge of the boundary layer than in a smooth wall boundary

layer. However, the mean profiles would be unaffected because the mean velocity is mostly associated with the laminar flow. It should be pointed out that the stress velocity inferred from the growth of the momentum thickness is 20% lower than those shown in Table 1. If these lower values of the stress velocities were used to normalize the Reynolds stress, our data would be more consistent with the hot-wire measurement throughout most of the boundary layer.

3.3. The heated turbulent boundary layer

Compared in Fig. 6 are some general features of the heated and unheated velocity boundary layers. Under the present experimental condition, the thermal layer is totally embedded in the velocity boundary layer, extending to only about 0.6 δ_u at the end of the test section. Therefore, the thermal layer is not fully developed. The growth of the thermal layer is correlated with $\delta_T = 0.38\ x^{0.63}$ (Fig. 6). This correlation is similar to $\delta_T \sim x^{0.8}$ for a slightly heated boundary layer. This would suggest that the turbulence mechanisms responsible for the transportation of the heated fluid into the boundary layer should be of the same character in both cases.

The gross effect of the wall heating is to thicken the velocity boundary layer. The displacement thickness is increased but the momentum thickness is reduced slightly (Table 1). The shape factor increase from about 1.6 at station 2 to 2.7 at station 8. These results are consistent with the results of Rotta[6].

Shown in Fig. 7. and 8 are the mean and rms fluctuation density profiles at stations 3, 5 and 7 . These profiles are quite consistent,

therefore the thermal layer can also be considered as self preserving. The mean density profiles were found to follow a logarithmic distribution. The rms density fluctuations are about ρ'/ρ_∞ = 2.0% at y/δ_T = 1.0, then increase to a maximum of 12% at y/δ_T = 0.15 and drop slightly towards the wall.

Since the thermal layer is self-preserving, these results can be compared with Townsend's[4] self-preserving analysis for velocity and temperature profiles in thermal layer. The equation for the velocity profile is the law of the wall (Eq. 1)

$$\frac{U}{u_\tau} = \frac{1}{K} \ln y^+ + C \qquad (1)$$

and the equation for the temperature profile is based on an analogous friction temperature, δ_T.

$$\frac{T_w - T}{\theta_\tau} = \frac{1}{K_\theta} \ln y^+ + C_\theta \qquad (2)$$

with K and C as the correlation coefficients. The friction temperature is defined by $\theta_\tau = Q_w/u_\tau$. Heat flux at the wall, Q_w, can be determined from the growth rate of the enthalpy thickness which is also equal to the Stanton number, S_T:

$$S_T = \frac{d\delta_h}{dx} = \frac{Q_w}{U_\infty(T_w - T_\infty)} \qquad (3)$$

The enthalpy thicknesses (Table 1) are found to increase linearly with x. The Stanton number, therefore, is constant over the test section and is equal to 2.3×10^{-3}. The corresponding Q_w is 35.3 m K/s, and θ_τ is about 40 K based on the stress velocity deduced from the mean velocity profiles (Table 1).

Temperature profiles corresponding to the density profiles of Fig.

8 are shown in Fig. 9 on the $(T_w - T)/\theta_\tau$ vs. y^+ plane. The significant density variation in the thermal layer is accounted for by the use of local viscosity in calculating y^+. These profiles are approximately linear for $y^+>50$ and are correlated using the values $K_\theta=0.8$ and $C_\theta=12.5$. In general, the slope of the profiles (K_θ) are consistent but the intercept (C_θ) seems to increase with increasing x. These values of K_θ and C_θ are much higher than those obtained in slightly heated boundary layers (values of $K_\theta=0.4$, $C_\theta=2.0$ were deduced by Antonia et al.[3]). Since Townsend's self-preserving analysis was developed for a slightly heated thermal layer with negligible density variation, our results demonstrated that his analysis can also be used to correlate this thermal layer with appreciable density variation. However, the physical significance of the differences in the values of K_θ and C_θ between the slightly heated and strongly heated cases can only be inferred from further experiments evidence.

The mean velocities are not drastically affected by strong wall heating. As shown in Fig. 10, the only difference between the heated and unheated profiles is that $_u$ for the heated case is larger. In contrast to our previous investigations of heated laminar and transitional turbulent boundary layers,[7,8,9] a particle free region next to the wall caused by thermophoresis[17] was not found. This can be explained by the insignificant effects of thermophoresis on LDV seed particles relative to that of inertia. Under the present experimental condition the thermophoretic velocity v_T close to the wall at $y/\delta_T = 0.05$ is only about 0.1 m/s, which is approximately 0.5% of U_∞. Hence, thermophoresis did not seem to affect our velocity measurements close to the heated wall.

Shown in Fig. 11 are the heated flow velocity profiles at stations 3, 5 and 7 on the u^+ vs. y^+ plane. Again, density variations in the thermal layer are taken into account by the use of local viscosity in evaluating y^+. For $y^+ > 70$ these profiles remain linear up to $y^+ = 500$. The data within this range are fitted with the law of the wall. The stress velocity corresponding to these profiles, (Table 1) are quite similar to those of the unheated case. However, the mean stress velocity inferred from the growth of the momentum thickness is only about 16% of the values shown in Table I.

This large discrepancy perhaps indicates that these stress velocities are just approximations and therefore not highly accurate. The stress velocity inferred from the growth of monentum thickness is associated with a large margin of uncertainty. This is because experimental uncertainties of density and velocity measurements are compounded by numerical integration when determining momentum thicknesses. The stress velocity inferred from the law of the wall correlation would not be totally consistent with stresses in the thermal layer because this method involves fitting data obtained inside and outside the thermal layer. Since turbulence in the outer region of the boundary layer obtains its energy from the wall region of the upstream part of the flow, the data outside of the thermal layer but within the velocity boundary layer is uncorrelated with shear stress at the heated wall. The reason for these stress velocities being so close to those of the unheated flow is that the thermal layer extends only to about 0.6 δ_u at station 9. For the practical purpose of comparing the data in the heated and unheated flows, these values are used to evaluate u_τ in Eq. 2, and to normalize the Reynolds stress data.

The rms fluctuation profiles shown in Fig. 12 are surprisingly similar to those of the unheated case, indicating that the total turbulence kinetic energy is not greatly affected by heat transfer from the wall. However, in Fig. 13, some effects are shown on the Reynolds stress profiles. In the outer region of the thermal layer, Reynolds stress levels remain comparable to those of the unheated case. Near the wall the Reynolds stress is reduced. The location where the heated profiles deviate from the unheated profiles scales with $y/\delta_T=0.5$ ($\rho/\rho_\infty \simeq 0.9$) and the level of reduction increases with increasing x. Our data can be interpreted to indicate a reduction of turbulence production in the inner region of the thermal layer. Since turbulence in the wall region is convected and transported to the outer region, it seems reasonable to conjecture that in a fully developed thermal layer the turbulence throughout the boundary layer would be reduced.

4. Discussion

Our data have shown that a reduction in Reynolds stress in the wall region is the only observable effect of strong wall heating on the turbulent boundary layer. This result would suggest a reduction in turbulence production without any change in turbulent kinetic energy. Unfortunately, our experimental data are insufficient to determine the ratio between turbulence production and dissipation in the heated boundary layer which would provide further insight into this phenomenon. Nevertheless, by showing the development of the thermal structures, the schlieren movies would provide some quantitative information on the thermal layer which would also be pertinent to the overall fluid motion and to the turbulence in the boundary layer. In a heated boundary

layer, the thermal structures should be closely associated with the large scale turbulent structures since the heated fluids are transported and convected by turbulence. These large scale structures were first observed by Kline et al[18] and their many aspects have been discussed by Willmarth[15] and also by Hinze.[16] These studies have shown that turbulence production in the wall region is relevant to the large scale turbulence structures. As shall be discussed later in this section, the quantitative information on the thermal structures can be interpreted with reference to the evolution of the large scale structures to propose a possible explanation for the reduction of Reynolds stress in the wall region.

The most striking feature of the heated boundary layer as shown by the schlieren images is that the development of the thermal structures in the boundary layer is cyclic. The cycles begin with the formation of blobs of heated gas at the edge of the otherwise thin (much less than δ_T) and quiescent thermal layer adjacent to the wall. These blobs grow in size, then form into streaks oblique to the wall and move outward as they are convected downstream. The streaks begin to break up when they reach farther out into the boundary layer and completely disappear in the outer region. This sequence of events is not always individually distinguishable and the blobs of heated fluid sometimes are found to merge or interact. It should be pointed out that the schlieren image is a result of integrated effect along the span of the heated boundary layer, therefore, the interaction and merging could be the superposition of several events taking place at different spanwise positions.

The cyclic development of the thermal structures seems to be asso-

ciated with the cyclic burst sequences which are related to the large turbulent structures in a turbulent boundary layer.[18] The bursting of low momentum fluid into the outer region is attributed to the lifting and eventual breaking-down of horse-shoe vortex loops generated by the interaction of in-rushing high-momentum fluid from the outer region with low momentum fluid in the sub-layer. In a heated boundary layer the general fluid motion would be the same except that the in-rushing fluid would be cold and the ejected fluid would be hot. The ejection of hot fluid from the wall is suggested by the trajectories of the thermal structures shown on the schlieren movies.

This general fluid motion is also consistent with the signs of the velocity-temperature cross-correlations measured by Antonia[3] et al. in slightly heated turbulent boundary layer. Near the heated wall, they found that $\overline{u\theta}$ and $\overline{v\theta}$ to be negative and positive respectively. We propose the following argument to explain these signs. In the in-rushing cold fluid, the cross-stream velocity and temperature are lower while the mean streamwise velocity is higher than their corresponding time-mean levels, therefore, v and θ are negative and u is positive. In the ejected hot fluid, the cross stream velocity and temperature are higher and streamwise velocity is lower than their time-mean levels, hence v and θ become positive and u becomes negative. As a result, the cross correlation $\overline{u\theta}$ would be negative and $\overline{v\theta}$ would be positive in both the in-rushing and ejected fluids. This simple argument is also consistent with the sign of Reynolds stress in the boundary layer.

The edge of the thermal layer, δ_T, therefore, essentially represents, on the average, the termination of the trajectories of the

ejected hot fluid bursts which constitute the basic mechanisms for transporting heat into the outer region of the velocity boundary layer. Based on these arguments it seems reasonable to suspect that the same general cyclic mechanisms should also govern the transport of momentum and heat in a fully developed thermal layer.

These qualitative features of the thermal and turbulence structures within the boundary layer suggest a possible explantion for the decrease in measured Reynolds stress. As discussed earlier, the interaction of fast in-rushing fluid from the outer region with slow moving fluid in the wall region is to create local shear layers close to the wall. The breaking-down of the vortex loops in the shear layers cause the eventual bursting. In a strongly heated boundary layer, the slow moving fluid adjacent to the wall is much hotter and more viscous than the in-rushing fluid. The interaction between the hot and cold fluid would be less vigorous and the vorticity in the local vortex loops would be lower than in the unheated flow. As a consequence, bursting would be less energetic. Since bursting contributes to about 70% of the Reynolds stress production, the overall Reynolds stress level near the wall would also be lowered. Because bursting is highly intermittent and occurs amid background turbulence, the overall time-mean rms fluctuations would not be greatly affected.

5. Conclusions

The effects of a stepwise jump in wall temperature of 800K on a fully developed turbulent boundary layer have been studied using Rayleigh scattering and laser Doppler velocimetry. The data reported in this paper include mean and rms fluctuation profiles of density for the

heated case, mean and rms fluctuation profiles of two velocity components and the Reynolds stress for both the unheated and heated cases. In addition, high speed schlieren movies of the heated boundary layer were made to obtain some quantitative information on the development of the thermal structures.

Under the present experimental condition of U_∞ = 19 m/s and T_w = 1100 K, the thermal layer is not fully developed and is completely embedded in the velocity boundary layer, attaining a thickness of only to 60% of $_u$ at the end of the test section. Mean and rms fluctuation profiles of both density and velocity are found to be self preserving at all the axial stations investigated. Temperature and streamwise velocity profiles are compared with the self preserving analysis developed by Townsend[4] with the density variation accounted for through the use of local viscosity to calculate the inner variable y^+. The velocity equation (Eq. 1) seems to be quite satisfactory for correlating the experimental data. However, the values of the correlation constants K and C for the temperature equation (Eq. 2) are different from those for a slightly heated turbulent boundary layer.

The velocity rms fluctuations appear to be unaffected by the wall heating. However, the Reynolds stresses are found to decrease in the thermal layer, and the level of reduction increases with increasing distance from the leading edge of the heated section. This apparent reduction in turbulence production with no overall change in turbulent kinetic energy level is discussed with reference to the structures of the thermal layer. From the schlieren movies, it appears that the convection and transport of heated fluid from the wall is associated with

the burst cycle. The interaction between cold fluid from the outer region with more viscous hot fluid close to the wall may possibly lead to a less energetic burst, and result in lowering of the Reynolds stress. However, in the absence of other supporting experimental data, this can only be reviewed as a tentative explanation for our observations. Further investigations are needed to proof its validity.

6. Acknowledgements

This work was supported by the Director, Office of Energy Research, Office of Basic Energy Sciences, Chemical Sciences Division of the U.S. Department of Energy under contract No. W-7405-ENG-48. Additional equipment supported by AFOSR Contract F 446 20-76-C-0083 through the Office of Research Services, University of California, Berkeley. The authors would like to thank Professor L. Talbot and Dr. F. Robben for their continued advice and support.

7. References

1. Johnson, D.S., J. Appl. Mech., Trans. ASME, 81, p. 225, (1959).

2. Blom, J., 4th Int'l Heat Tranf. Conf. Paris, Paper No. FC 2.2 (1970).

3. Antonia, R.A., Danh, H.Q. and Prabhu, A., J. Fluid Mech., 80, 1, p. 153 (1977).

4. Townsend, A.A., J. Fluid Mech., 22, p. 779 (1965).

5. Nicholl, C.I.H., J. Fluid Mech., 40, 2, p. 361 (1970).

6. Rotta, J.C., Warme-und-Staffubertragung, 7, p. 133 (1974).

7. Schefer, R.W., Robben, F. and Cheng, R.K., Combustion and Flame, 38, 1, p. 51 (1980).

8. Cheng, R.K., Bill, R.G., Jr., and Robben, F., 2nd Symp. on Turbulent Shear Flows, p. 3.18 (1979).

9. Cheng, R.K., Bill, R.G., Jr., and Robben, F., 18th Symp. (Int'l.) on Combustion, The Combustion Institute, p. 1021 (1981).

10. Ng, T.T., Ph.D. Thesis, Department of Mechanical Engineering, University of California, Berkeley, (1981).

11. Duranni, T.S. and Greated, C.A., Laser System in Flow Measurement, Plenum Press, New York (1977).

12. Durst, F., Popp, M. and Tropea, C.D., SFB, Report (1980).

13. Demotakis, P.E., Collins, D.J. and Land, D.B., Laser Velocimetry and

Particle Sizing, Hemisphere Publication Corporation, Washington, p. 208 (1979).

14. Cheng, R.K. and Ng, T.T., First Specialist Meeting (International) of the Combustion Institute, The Combustion Institute, 1, p. 13 (1981).

15. Willmarth, W.W., Advances in Applied Mechanics, 15, p. 159 (1975).

16. Hinze, J.O., Turbulence, McGraw Hill, New York (1975).

17. Talbot, L., Cheng, R.K., Schefer, R.W. and Willis, D.R., J. Fluid Mech., 101, p. 737 (1980).

18. Kline, S.J., Reynolds, W.C., Schwaub, F.A., J. Fluid Mech., 30, 4, p. 741 (1967).

19. Corrsin, S. and Kistler, A.L., Natl. Advisory Comm. Aeronaut. Tech. Notes 3133 (1954).

20. Klebanott, P.S., Natl. Advisory Comm. Aeronaut. Tech. Notes 3178 (1954).

Table 1

	Unheated Boundary layer						Heated Boundary Layer						
Station	x (mm)	δ_u (mm)	δ_m (mm)	δ_d (mm)	u_τ (m/s)	H	δ_u (mm)	δ_T (mm)	δ_m (mm)	δ_d (mm)	δ_h (mm)	u_τ (m/s)	H
1	10.0	12.0	0.989	1.492	0.909	1.508	12.0						
2	35.0	12.0	1.030	1.614		1.566	12.5	3.4	1.020	1.615	0.095		1.582
3	69.0	12.8	1.119	1.673	0.910	1.494	14.0	5.4	1.016	1.895	0.151	0.891	1.865
4	94.0	12.0	1.182	1.755		1.486	13.0	6.6	1.016	2.141	0.239		2.107
5	120.0	12.0	1.190	1.782	0.909	1.497	15.2	7.5	1.062	2.319	0.306	0.883	2.184
6	155.0	13.0	1.184	1.767		1.493	15.6	8.6	1.057	2.483	0.358		2.350
7	183.0	14.0	1.267	1.887	0.892	1.489	16.0	10.0	1.020	2.664	0.433	0.879	2.608
8	203.0	13.0	1.278	1.905		1.491	16.0	10.6	1.012	2.737	0.488		2.705
9	230.0							11.0					

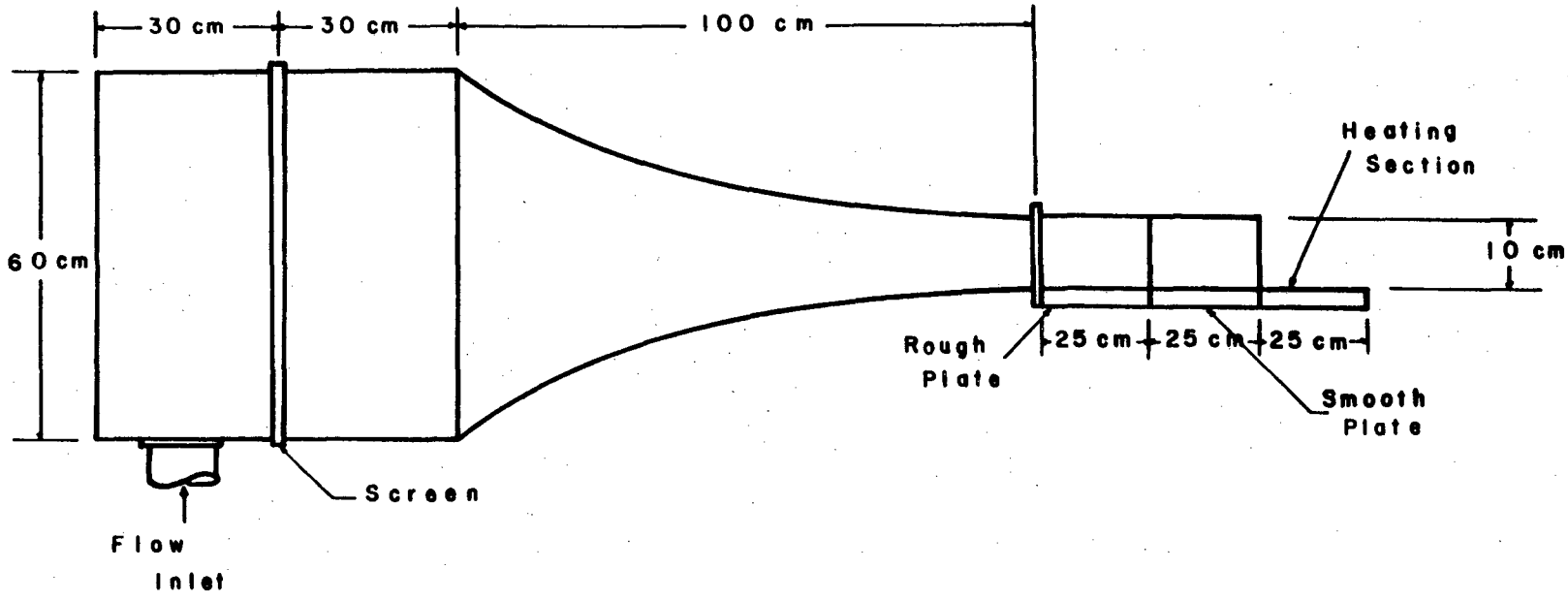

Fig. 1 Schematics of the experimental system.

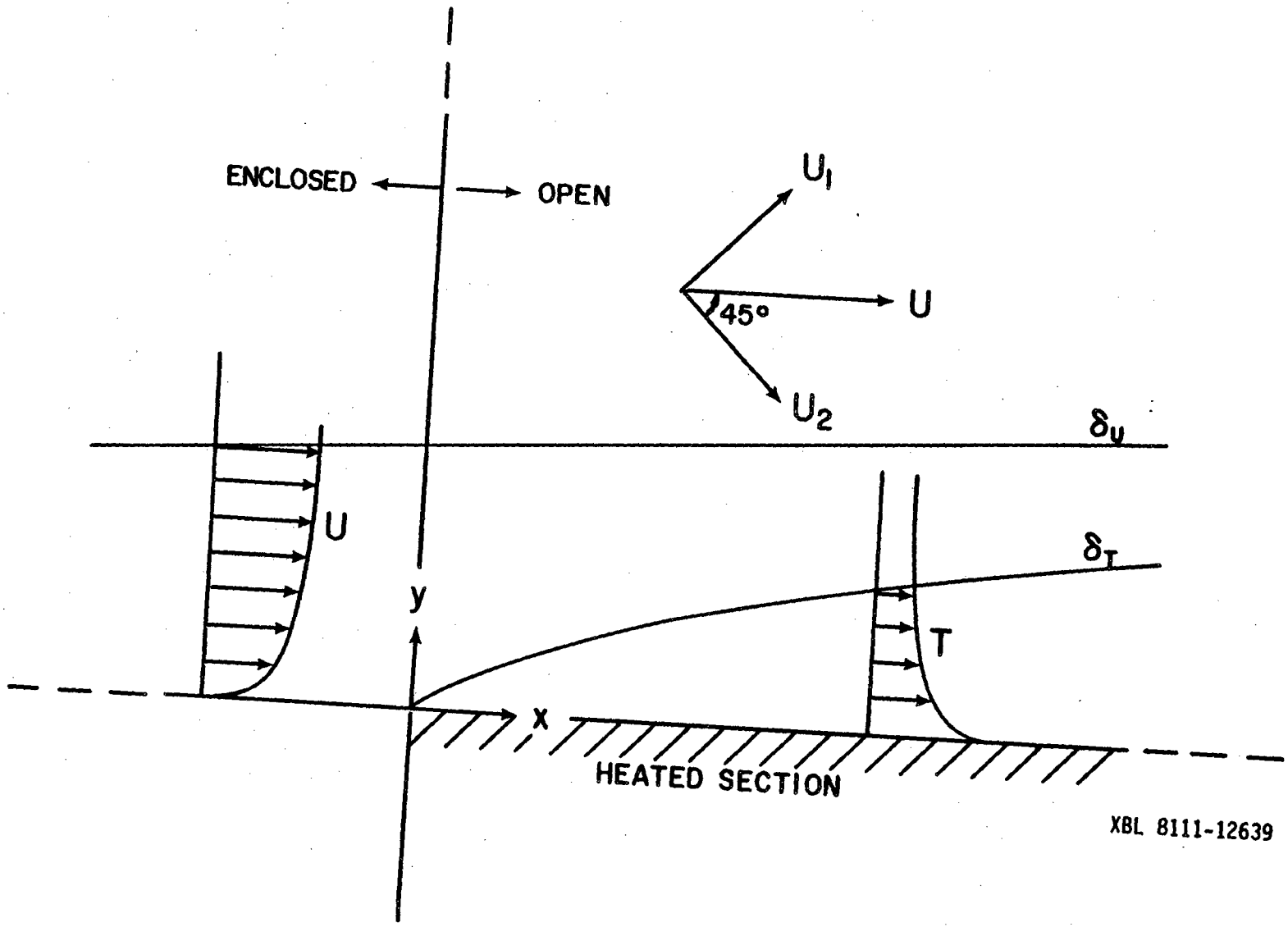

Fig. 2 Co-ordinate system and orientations in the test section.

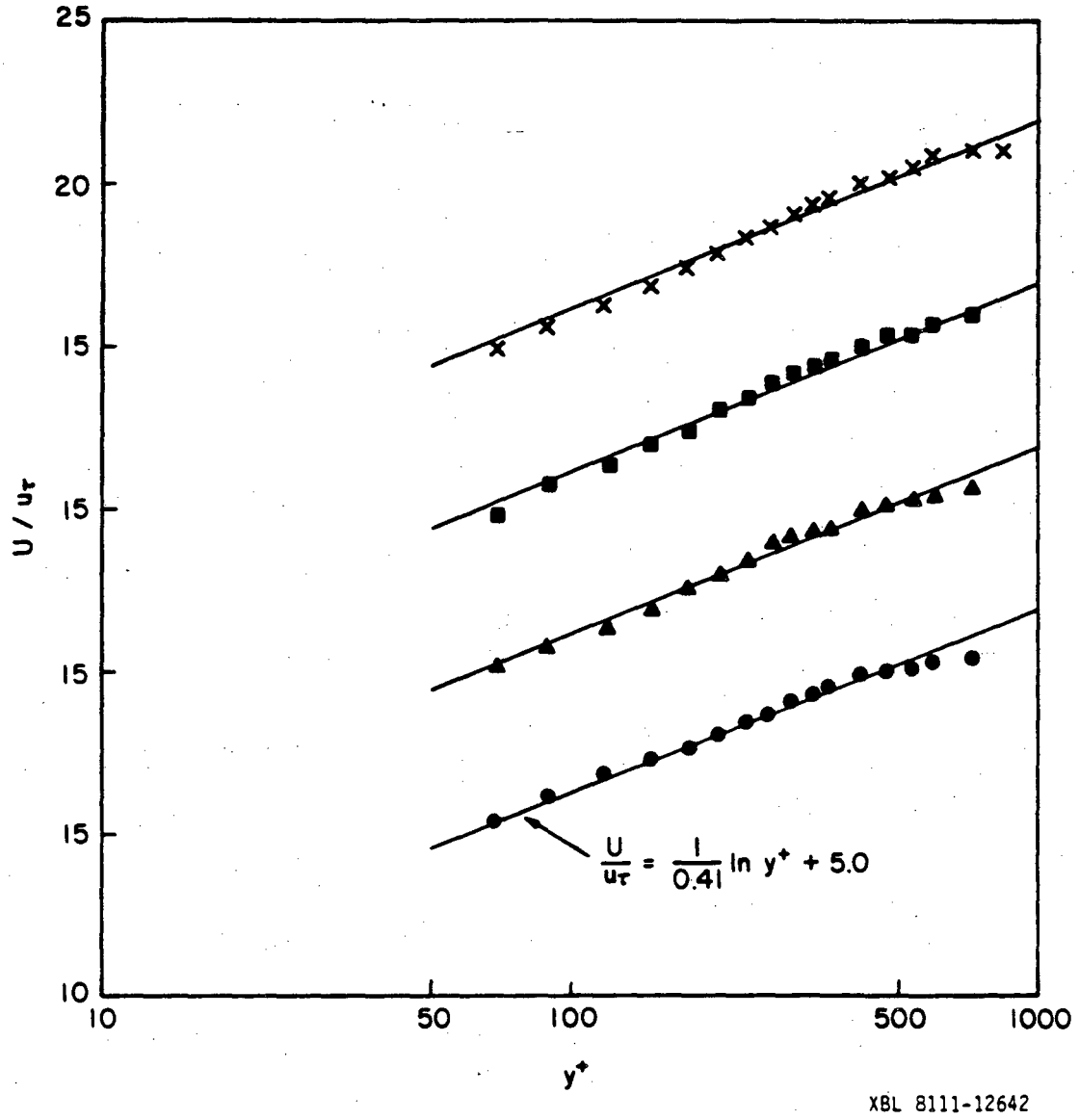

Fig. 3 Streamwise velocity profiles in the unheated boundary layer at station 1, O ; 3, Δ ; 5, □ ; and 7, × .

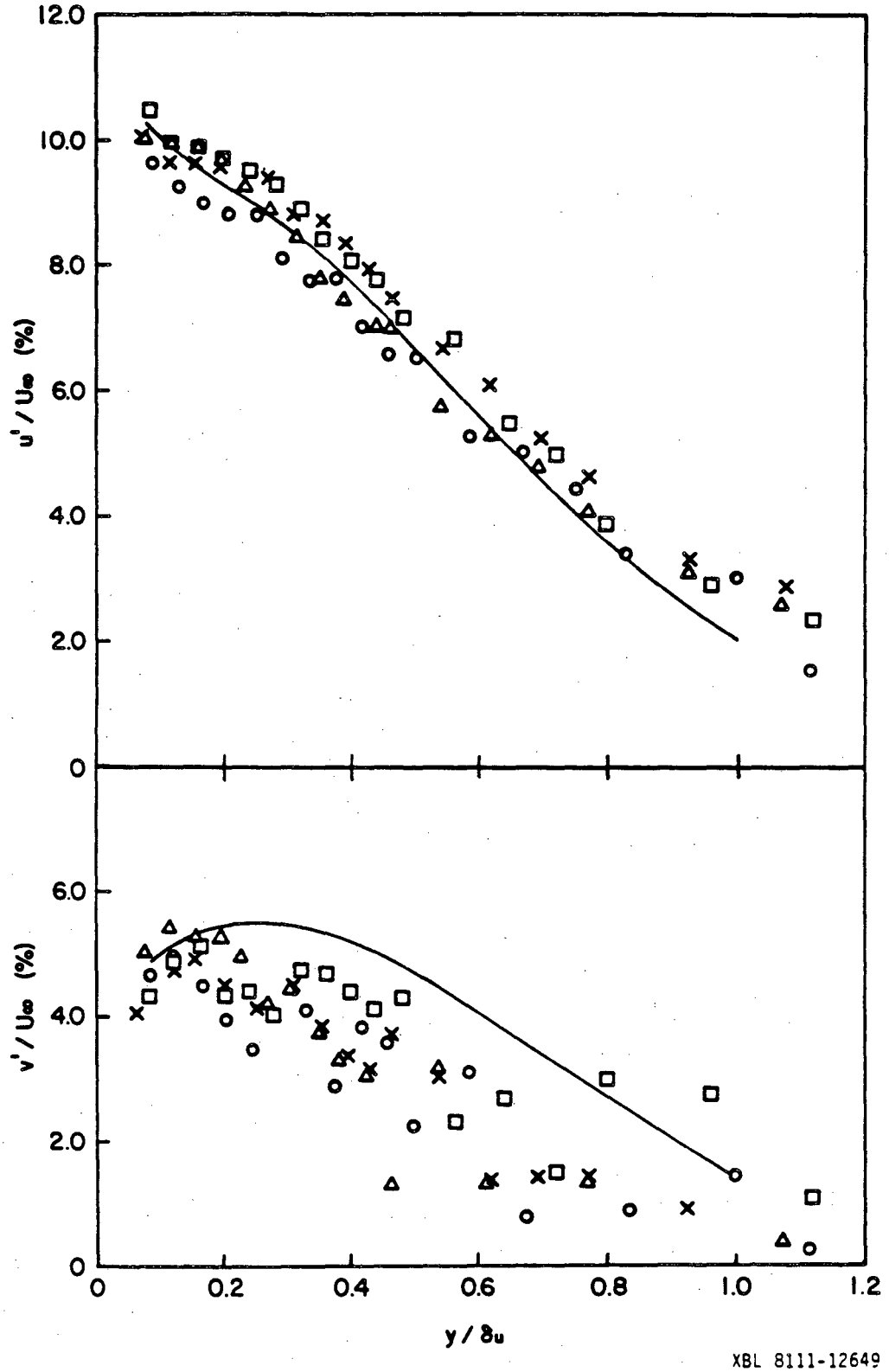

Fig. 4 RMS fluctuation profiles in the unheated boundary layer at stations 1, ○ ; 3, △ ; 5, □ ; and 7, × .

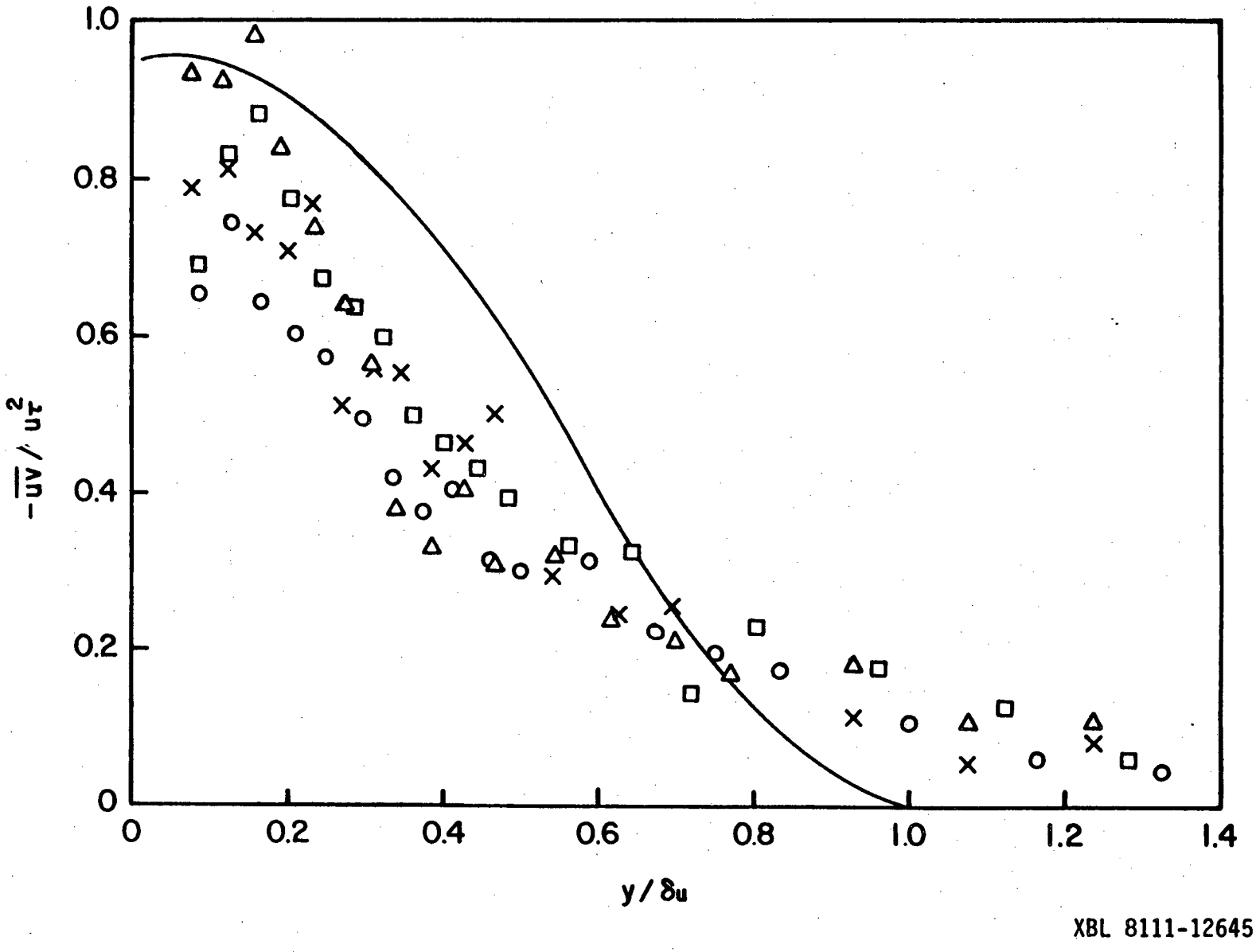

Fig. 5 Reynolds stress profiles in the unheated boundary layer at stations 1, O ; 3, Δ ; 5, □ ; and 7, × .

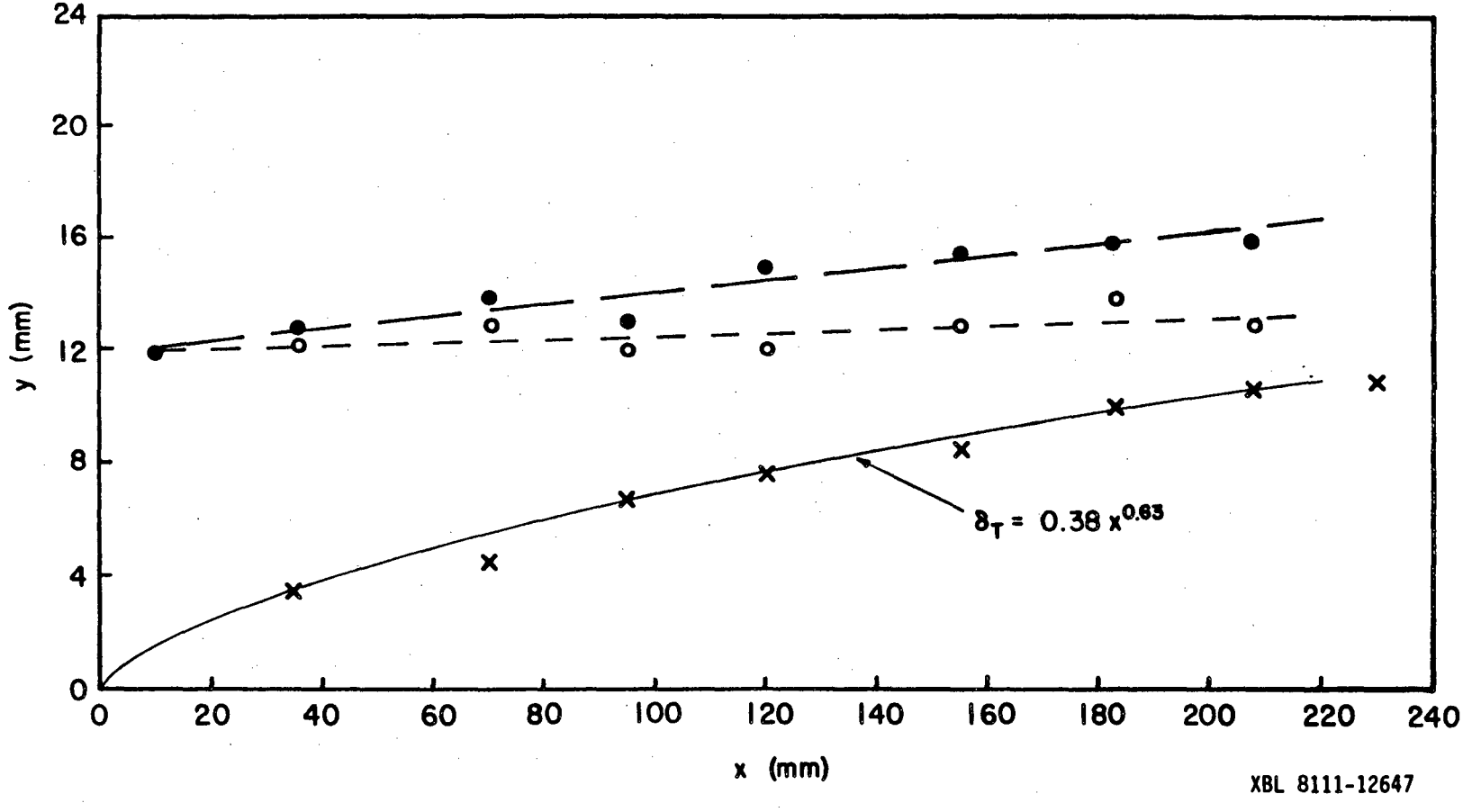

Fig. 6 Comparison of heated and unheated boundary layers; O , unheated δ_u ; ● , heated δ_u; × , δ_T.

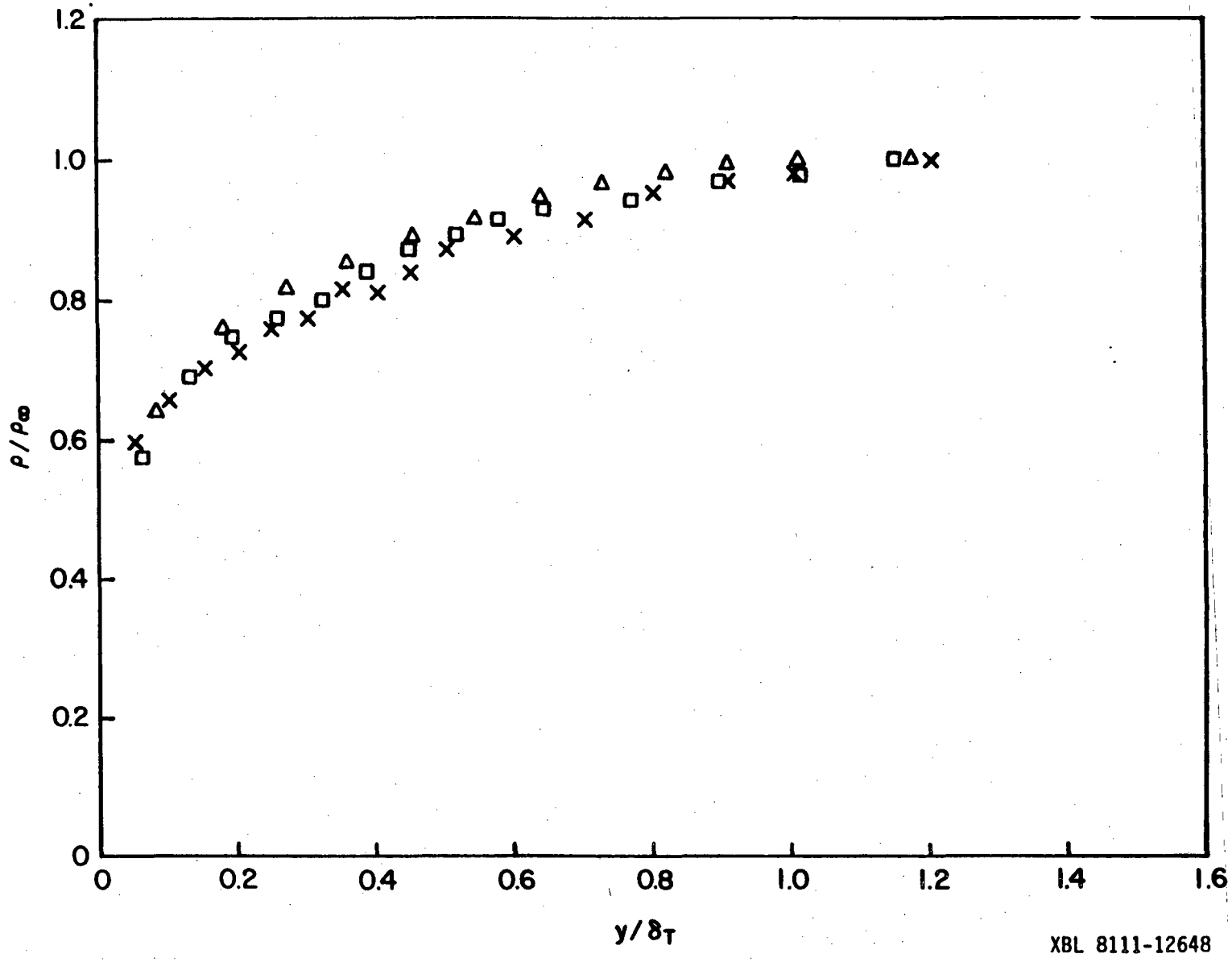

Fig. 7 Mean density profiles at stations 3, △ ; 5, □ ; and 7, × .

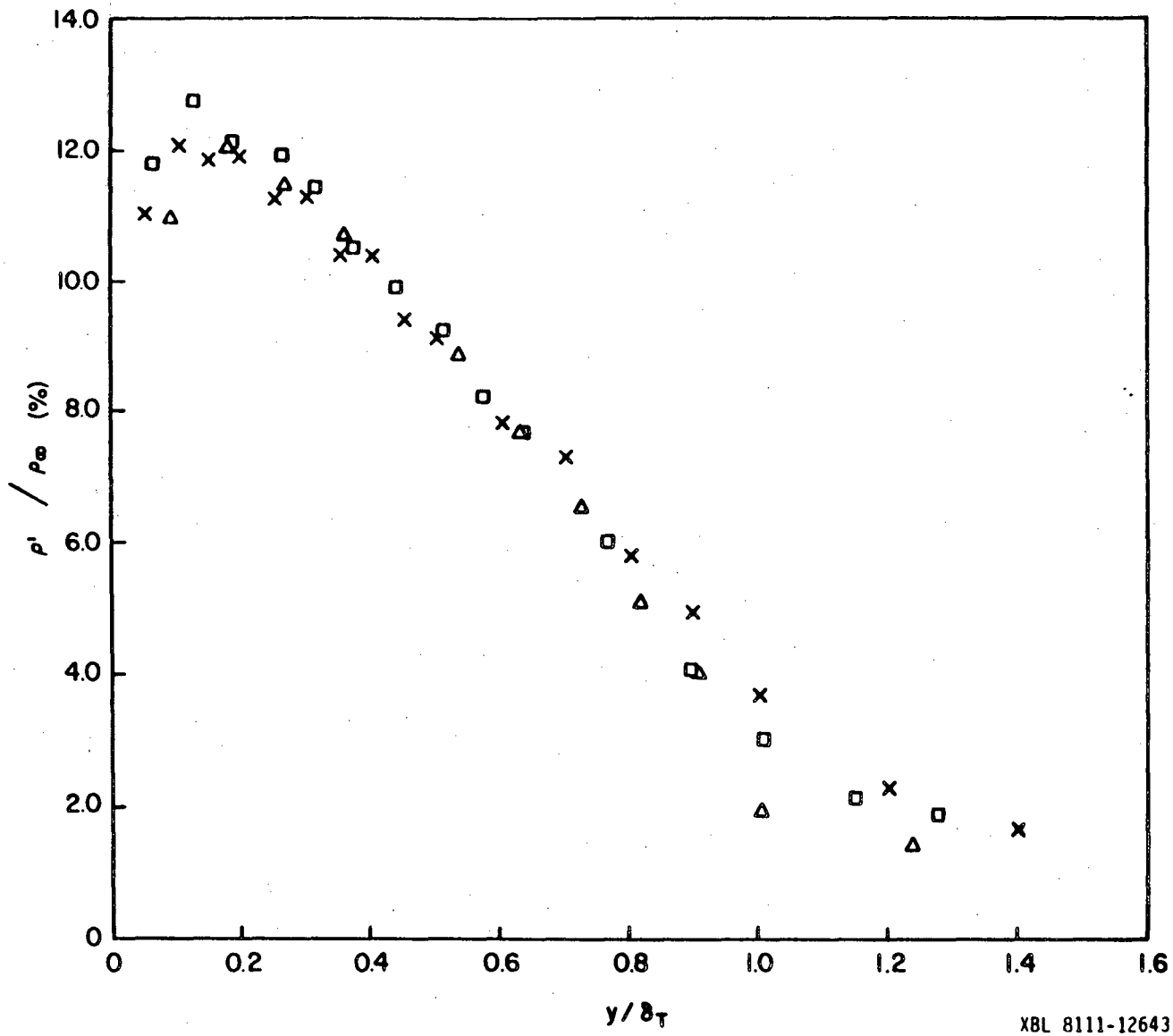

Fig. 8 RMS density fluctuation profiles at stations 3, △ ; 5, □ ; and 7, × .

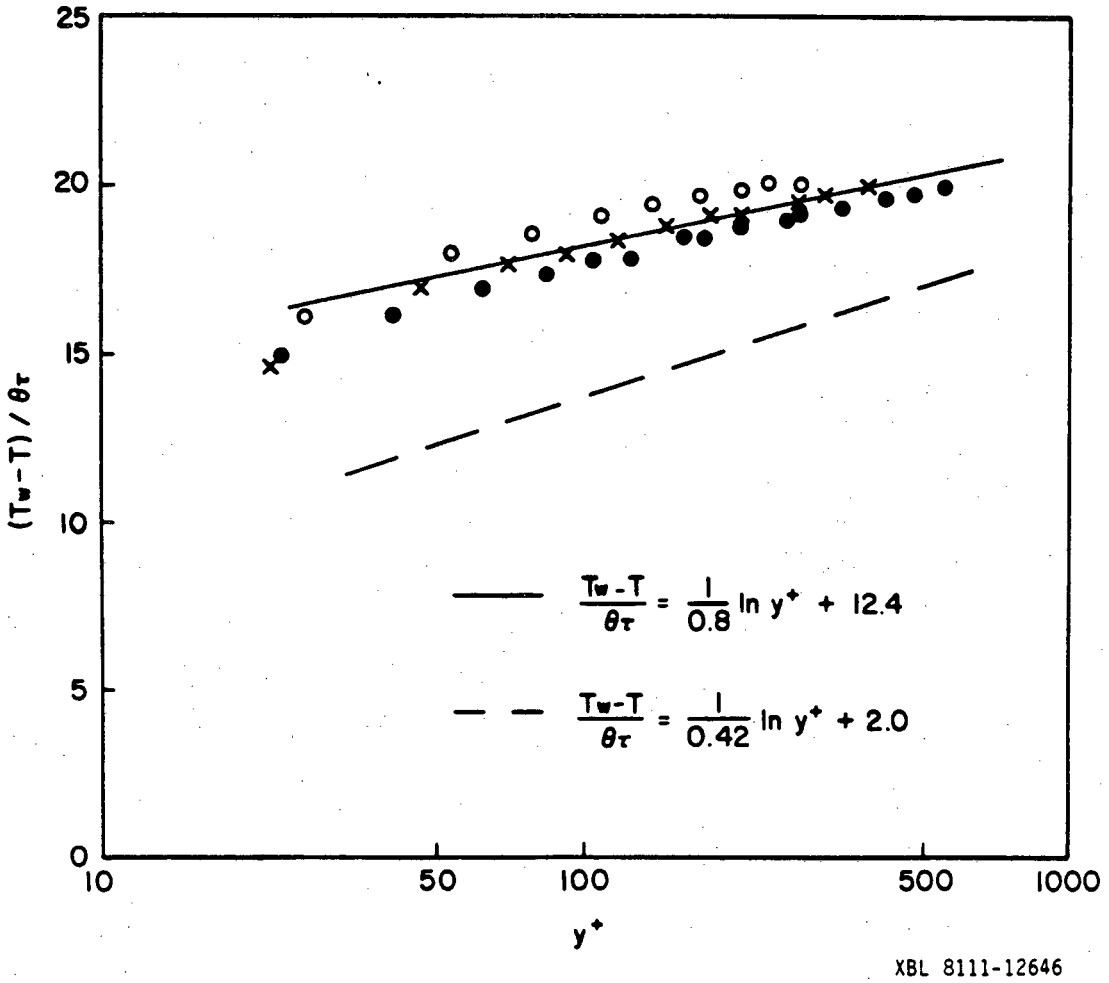

Fig. 9 Mean temperature profiles at stations 3, O ; 5, × ; and 7, ● .

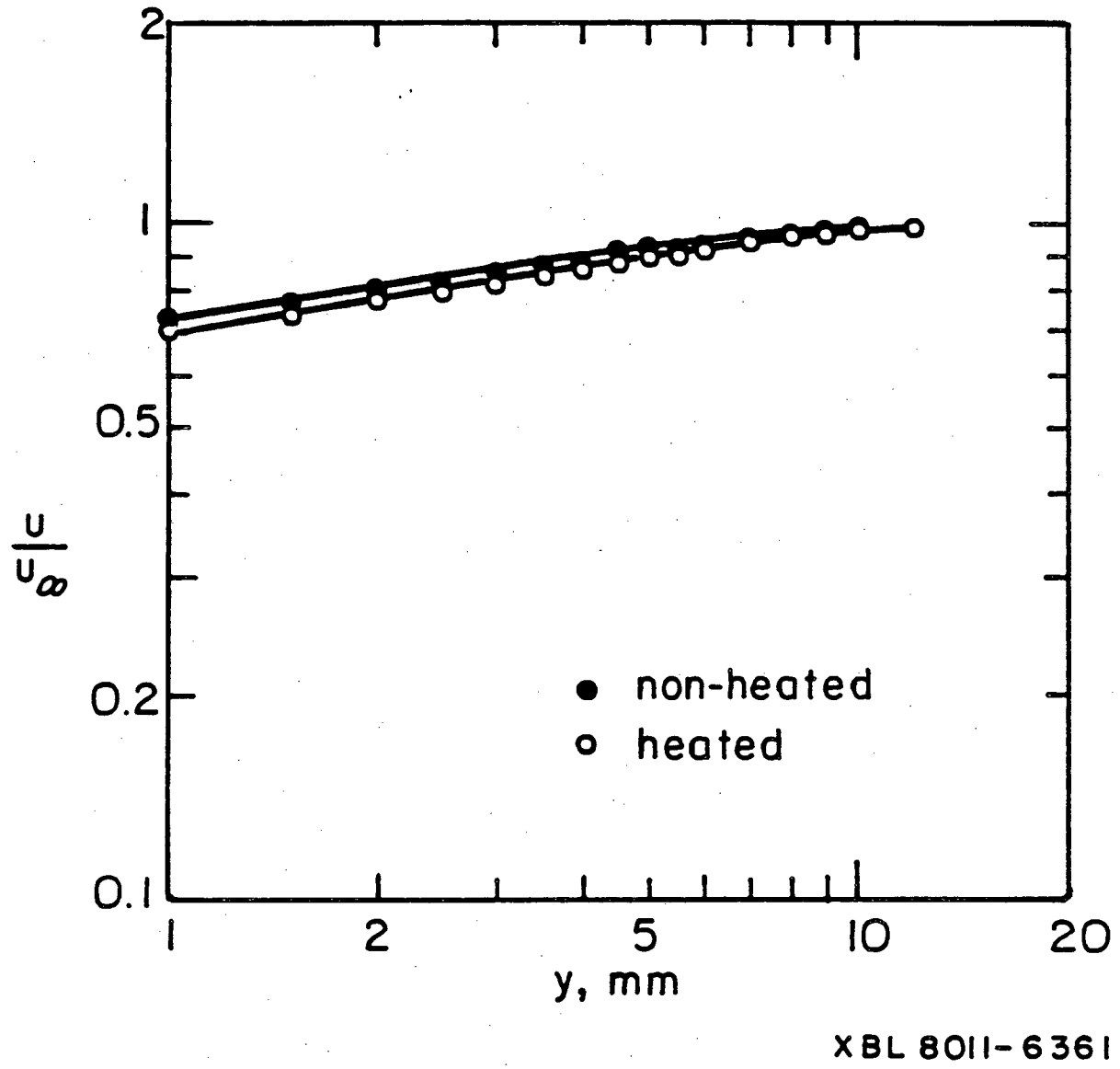

Fig. 10 Comparison of heated and unheated velocity profiles at station 3.

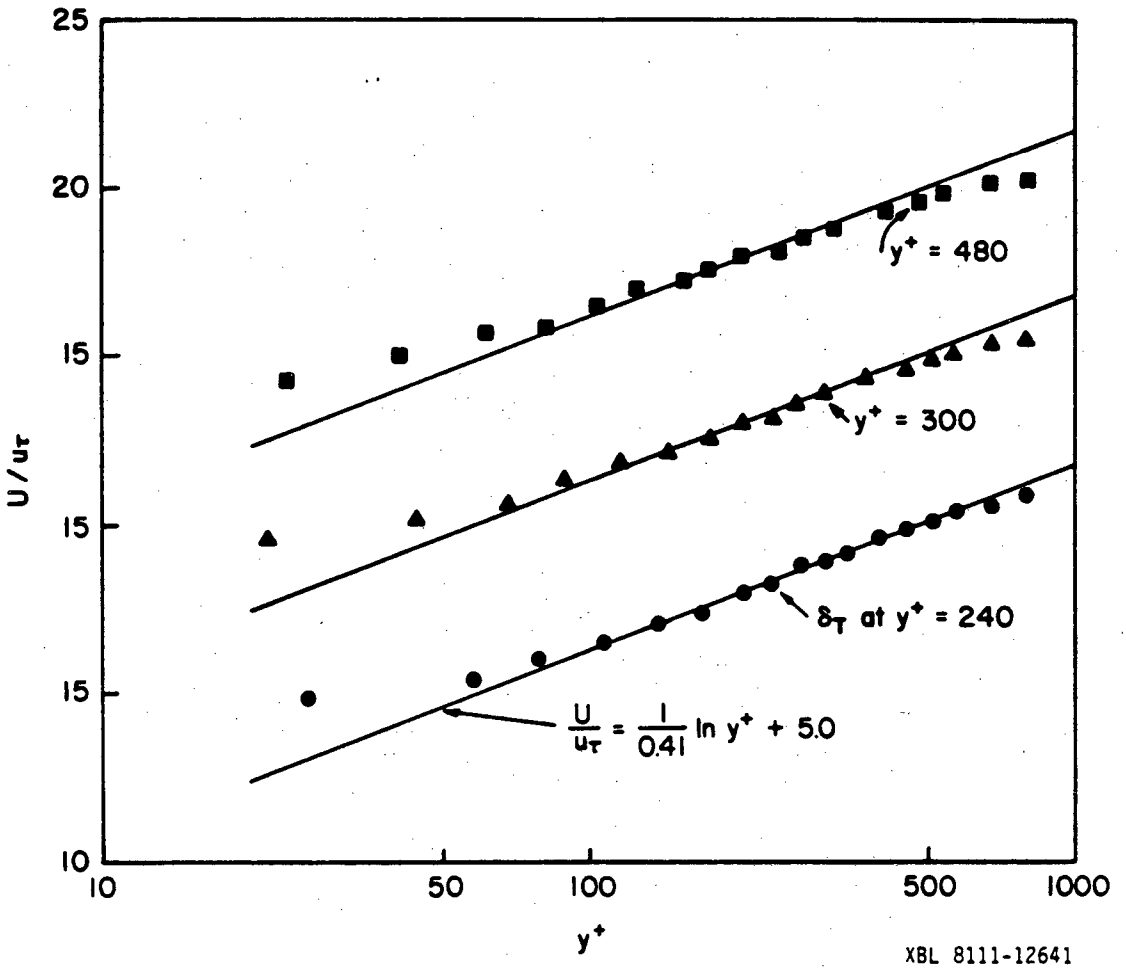

Fig. 11 Streamwise velocity profiles in heated boundary layer at stations 3, ● ; 5, ▲ ; and 7, ■ .

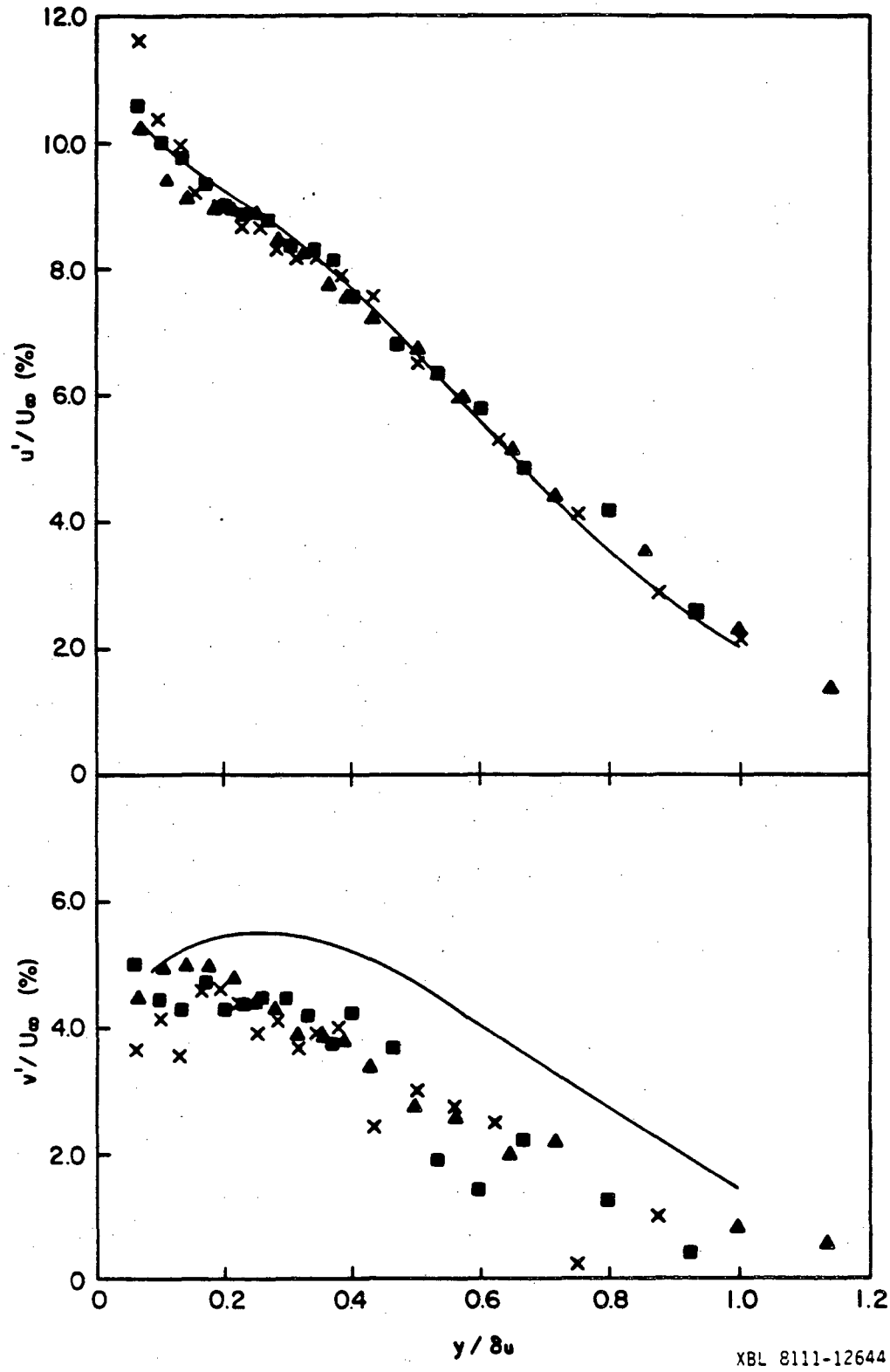

Fig. 12 RMS velocity fluctuation profiles in heated boundary layer at stations 3, ▲ ; 5, ; and 7, ✕ .

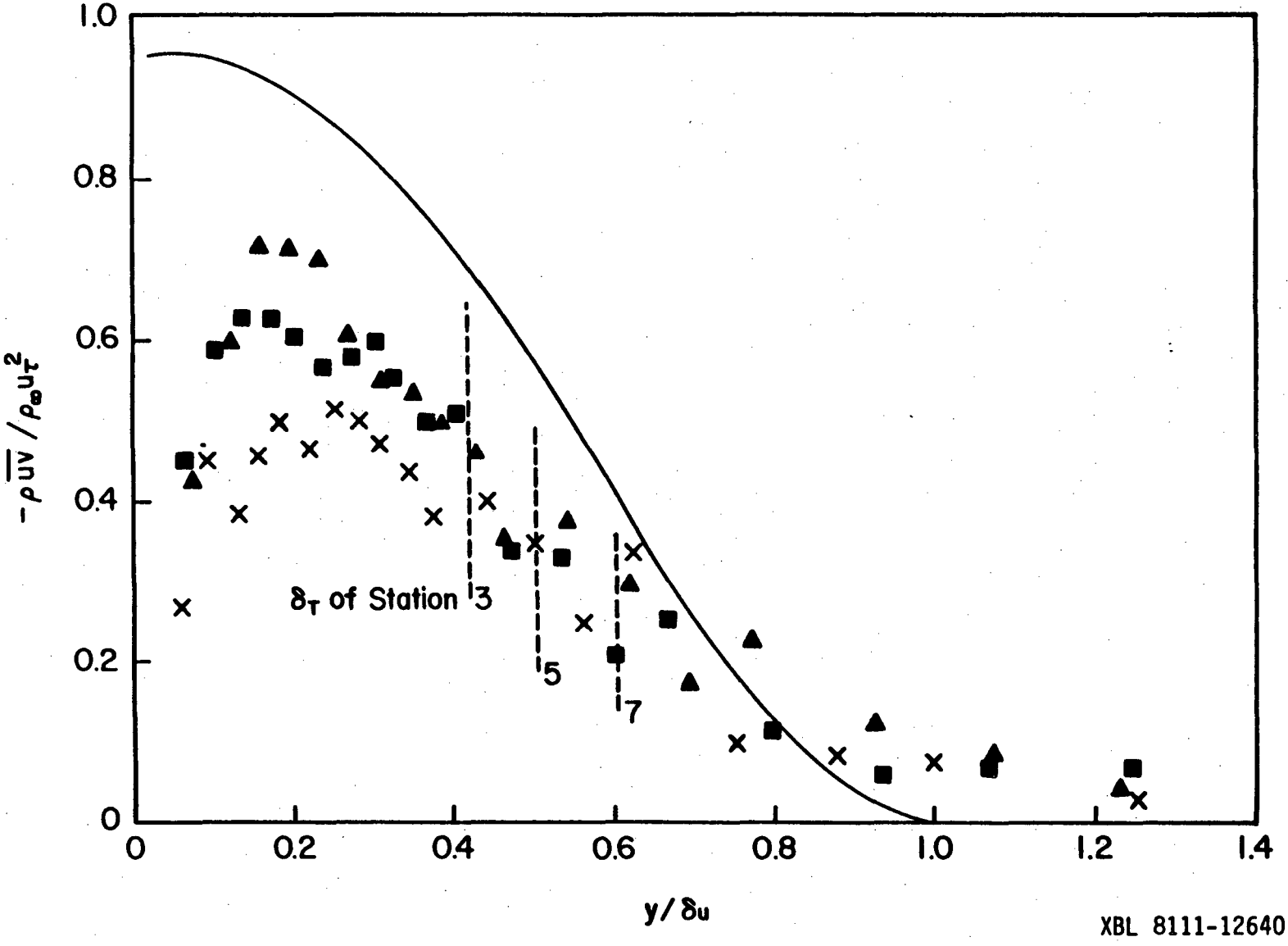

Fig. 13 Reynolds stress profiles in heated boundary layer at stations 3, ▲ ; 5, ; and 7, × .

This report was done with support from the Department of Energy. Any conclusions or opinions expressed in this report represent solely those of the author(s) and not necessarily those of The Regents of the University of California, the Lawrence Berkeley Laboratory or the Department of Energy.

Reference to a company or product name does not imply approval or recommendation of the product by the University of California or the U.S. Department of Energy to the exclusion of others that may be suitable.

TECHNICAL INFORMATION DEPARTMENT
LAWRENCE BERKELEY LABORATORY
UNIVERSITY OF CALIFORNIA
BERKELEY, CALIFORNIA 94720